

Validation of a Secondary Fabric Supplier and Characterization of Alternate Cores for use in the Aptera 2e Sandwich Core Composite

Bryan Rogers

California Polytechnic State University, San Luis Obispo

Department of Materials Engineering

Advised by Dr. Blair London

In partnership with Aptera Motors

June 4th, 2010

Approval Page

Project Title: Validation of a Secondary Fabric Supplier and Characterization of Alternate Cores for use in the Aptera 2e Sandwich Core Composite

Author: Bryan J. Rogers

Date Submitted: June 4th, 2010

CAL POLY STATE UNIVERSITY
Materials Engineering Department

Since this project is a result of a class assignment, it has been graded and accepted as fulfillment of the course requirements. Acceptance does not imply technical accuracy or reliability. Any use of information in this report is done at the risk of the user. These risks may include catastrophic failure of the device or infringement of patent or copyright laws. The students and staff of Cal Poly State University, San Luis Obispo cannot be held liable for any misuse of the project.

Prof. Blair London
Faculty Advisor

Signature

Prof. Trevor Harding
Department Chair

Signature

Abstract

Polymer matrix composites' high strength to weight ratio has made them an ideal material choice for use in lightweight transportation vehicles. Aptera Motors, a company based out of Oceanside, CA, is currently developing a next-generation high efficiency passenger vehicle called the Aptera 2e. The 2e's body is composed of a sandwich core composite containing laminates of E-glass fibers embedded within an epoxy matrix sandwiched between a polyester hexagonal core. This project looked to validate a secondary fabric supplier for use in Aptera's composite and characterize the core shear properties of two alternate core materials for future iterations of Aptera's vehicle. Validation of the secondary fabric supplier was achieved by experimentally determining and comparing the tensile strength and modulus, in-plane shear strength, and short-beam strength of laminates containing Aptera's current fabric (Vectorply) and alternate fabric (Saertex). All mechanical testing followed appropriate ASTM standards (D3039, D3518, D2344). Using a two sample t-test, the mechanical properties of the laminates were determined to be statistically different. Laminates that contained Saertex fabrics had a greater mean tensile strength and modulus than laminates with Vectorply fabrics (95% CI: 7-29 MPa and 0.3-1.5 GPa, respectively). The mean short beam strength of laminates containing Saertex fabrics was also statistically greater than those containing Vectorply fabrics (95% CI: 4.6-7.3 MPa). Fracture surfaces of the two fibers were examined with a scanning electron microscope to qualitatively compare the adhesion at the fiber-matrix interface. Fibers within Saertex fabrics appeared to have greater adhesion at the fiber-matrix interface compared to Vectorply. Characterization of the alternate core materials was accomplished by measuring the core shear strength and flexural modulus of the composite in three-point bending following ASTM C373. The mechanical properties of the two alternate cores (TF2, LRC3) were compared to Aptera's current core material (XF6). The TF2 core exhibited a greater mean core shear strength than XF6 (95% CI: 0.77-0.96 MPa), while LRC3 was less than XF6 (95% CI: 0.25-0.45 MPa). There was no statistical difference between the flexural modulus of the XF6 and TF2 cores, whereas LRC3's flexural modulus was statistically less than XF6 (95% CI: 0.35-0.87 GPa). The difference in core shear properties was attributed to the varying amount of resin uptake of the various cores during the fabrication process.

Key Words: materials engineering, polymer matrix composite (PMC), sandwich core composite, Aptera Motors, laminate, E-glass fiber, polyester hexagonal core, epoxy resin, scanning electron microscopy, fiber-matrix adhesion.

Acknowledgements

This project would not have been possible without the funding of Aptera Motors, Oceanside, CA. I would like to thank Krista Anderson, Aptera's composite engineer, for her time spent fabricating the test samples and direction provided in helping me complete my senior project. I would also like to thank my advisor Dr. Blair London of the Materials Engineering department at California Polytechnic State University in providing technical support and guidance. Finally I would like to thank Noah Hansen for his moral and technical support.

Table of Contents

1. Introduction	1
1.1 Aptera 2e Vehicle.....	1
1.2 Broader Impacts.....	2
1.2.1 Environmental Advantages of the 2e.....	2
1.2.2 Production of the 2e	3
1.2.3 Safety of the 2e	3
1.3 General Background on Polymer Matrix Composites.....	4
1.3.1 Applications of PMCs in the Transportation Industry.....	5
1.4 Manufacturing of Polymer Matrix Composites	7
1.4.1 Aptera 2e’s PMC Structure.....	7
1.5 Project Objectives	10
1.5.1 Saertex Fabric.....	11
1.5.2 Alternate Core Materials.....	11
2. Experimental Procedures.....	13
2.1 Experimental Procedure used in the Validation of Saertex Fabrics.....	13
2.1.1 Determination of In-plane Tensile Strength and Modulus	13
2.1.2 Determination of In-plane Shear Strength	14
2.1.3 Determination of Short-Beam Strength.....	15
2.2 Characterization of Alternate Core Materials.....	16
2.2.1 Determination of the Core Shear Strength.....	17
2.2.2 Determination of Flexural Modulus.....	17
2.3 Scanning Electron Microscopy	18
3. Results and Statistical Analysis	20
3.1 Results of Secondary Fabric Validation.....	20
3.1.1 Tensile Test Results.....	20

3.1.2 Short-Beam Strength Results	22
3.1.3 In-Plane Shear Strength Results.....	23
3.1.4 Laminate Density Calculations	24
3.2 Results of Alternate Core Characterization	25
3.2.1 Core Shear Strength Results	25
3.2.2 Flexural Modulus Results	28
3.2.3 Core Density Calculations	29
3.3 Scanning Electron Microscopy Results	29
4. Discussion.....	31
5. Conclusions	35
6. Recommendations	35
7. Work Cited	36

List of Figures

Figure 1: Revolutionary design of the Aptera 2e vehicle that utilizes a sandwich core composite body to reduce the weight of the vehicle thus increasing the fuel efficiency.	1
Figure 2: Top view of the Aptera 2e showcasing the solar cells on the roof of the vehicle that power the car's climate control system.	2
Figure 3: Schematic of a PMC showing the fiber reinforced face sheets "sandwiching" the honeycomb core.	4
Figure 4: The Ultralite, a 1992 GM concept car, had a curb weight of 1400 lbs. The carbon-fiber body structure was built by Scaled Composites Co. and the vehicle contained a 1.5L, 111 hp engine.	6
Figure 5: Schematic of Vectorply's preform fabric utilized in Aptera's fiber reinforced face sheets.	8
Figure 6: Lantor's Soric XF6 core which consists of a polyester hexagonal core structure separated by resin flow channels to allow for a homogenous dispersion of resin during the fabrication of a sandwich core composite.	9
Figure 7: Stacking sequence of Aptera's sandwich core composite within the vacuum-assisted resin transfer mold.	9
Figure 8: Photograph of Lantor's Soric LRC core material. The honeycomb cell structure is 4.3x larger than XF6's structure causing the composite to uptake less resin during the resin infusion process.	12
Figure 9: Lantor's Soric TF core that consists of a dot-printed cell structure. This core is typically paired with another core material to achieve adequate core properties.	12
Figure 10: Schematic of an in-plane shear sample showing the fibers orientated +/- 45° to the length of the sample.	14
Figure 11: Schematic side view of a short-beam strength sample loaded in a 3-point bend test fixture. The span length is a function of the thickness (h).	16
Figure 12: Schematic of a core shear sample showing the core thickness and the sandwich thickness. The width of the sample (b) would be going into the page.	17
Figure 13: Representation of how the slope of the first linear region was calculated using points at 1.00 and 2.00 mm deflection.	18
Figure 14: Graphical comparison of the two fabric supplier's tensile strength. The mean tensile strength of each supplier is indicated by the cross-hair mark on the graph.	20
Figure 15: Statistical boxplot comparing the variation in the tensile modulus of the two fabric suppliers. The mean tensile modulus is identified by the cross-hair mark on the plot.	21

Figure 16: Failed Vectorply short-beam strength sample due to interlaminar shear shown by the red arrow.....	22
Figure 17: Statistical comparison of Vectorply and Saertex’s short-beam strength. The mean is denoted by the cross-hair symbol while outliers are denoted with an asterisk.....	22
Figure 18: Boxplot comparing the in-plane shear strength of the two fabric suppliers. The Saertex fabrics exhibited shear strengths that were nearly two times that of Vectorply.	23
Figure 19: Boxplot comparing the core shear strength of the three core materials. Some samples of the LRC3 and TF2 cores were excluded from the boxplot due to unacceptable failure modes.....	25
Figure 20: Side view of the three acceptable failure modes observed during the core shear testing: (a) core-to-facing failure; (b) explosive core failure; (c) transverse core shear failure. Red arrows denote failure locations.	26
Figure 21: Top view photograph of a LRC3 core that experienced a facing failure before core failure during the core shear testing. The failure occurred on the top face sheet directly under the loading nose.	26
Figure 22: Pareto chart displaying the failure modes experienced by the TF2 samples using ASTM C393 failure code. DAT stands for a special failure case in which the core-to-facing failure occurred directly beneath the loading nose.	27
Figure 23: Pareto chart of the failure modes experienced by the LRC3 samples following ASTM C393 failure code.	27
Figure 24: Comparison of the three cores’ flexural modulus. The crosshair represents the mean flexural modulus.	28
Figure 25: SEM micrographs of epoxy matrix composite containing E-glass fibers: (a) Vectorply fibers (b) Saertex fibers. The Saertex fibers are outlined in green and purple to better identify them.....	30
Figure 27: Silane coupling agent that has a silicon bonded to a functional group (R) which is compatible with the epoxy matrix. The inorganic material is the E-glass fiber, while the organic material is the epoxy resin.	32

List of Tables

Table I: Properties of Typical Fiber Reinforced Composite Materials and Structural Metals	4
Table II: E-Glass Fiber Content in Vectorply's E-QX 2600 and E-QX 3600 Fabrics ¹⁴	8
Table III: Mechanical Properties Required for the Aptera 2e FEA Model.....	10
Table IV: Summary of Laminate Tensile Test Results	21
Table V: Mass per Surface Area and Specific Mechanical Properties of the Two Fabric Suppliers.....	24
Table VI: Mass per Surface Area of the Core Materials Characterized.....	29
Table VII: Summary of Vectorply and Saertex Mechanical Properties	31

1. Introduction

1.1 Aptera 2e Vehicle

The Aptera 2e is a next generation high-efficiency passenger vehicle. The car is a battery electric three wheel automobile designed to be as safe as the average sedan, while being more fuel efficient and sustainable (Figure 1). In order to make the car safe and efficient the vehicle's cabin is constructed of a proprietary polymer matrix sandwich core composite. The composite provides an impact-resistant exterior that is lighter than steel and three times as strong. Combined with integrated high strength aluminum door beams, the car has the ability upon impact to transfer loads into the body and away from the cabin, thus protecting its passengers in the event of an accident. In addition, the vehicle comes with driver and passenger airbags and a front impact zone designed after systems employed to protect race car drivers¹.



Figure 1: Revolutionary design of the Aptera 2e vehicle that utilizes a sandwich core composite body to reduce the weight of the vehicle thus increasing the fuel efficiency.

According to Aptera, the 2e can accelerate from 0-60 mph in 9 seconds and is capable of reaching speeds in excess of 90 mph. The 2e can seat two adults in addition to having 22.75 ft³ of cargo room (Aptera estimates that the vehicle can carry 15 bags of groceries, a couple of surfboards, or multiple sets of golf clubs)¹. The vehicle is equipped with smart phone connectivity; allowing owners to play music and receive calls through the car's stereo system. The vehicle also has a radio, CD/DVD/MP3 player, and GPS navigation system that are integrated into an in-console touch screen "carputer." The vehicle has a solar assisted climate control system which utilizes solar cells situated on the car's roof that ensures the vehicle is at an adequate temperature at all times¹. The vehicle incorporates a rear vision system that displays what is occurring behind the vehicle on a centralized screen that is easily viewable for the driver;

this feature combined with adjustable side mirrors helps eliminate “blind spots” experienced in the average sedan.

1.2 Broader Impacts

1.2.1 Environmental Advantages of the 2e

The airfoil design of the 2e is intended to reduce the car’s drag coefficient as it moves forward, thus increasing the vehicle’s fuel efficiency. Aptera claims that the vehicle has a drag coefficient of 0.15, which is comparable to the drag coefficient that Lance Armstrong experiences while biking in the Tour de France¹ (the average automobile has a drag coefficient between 0.30-0.35²). The vehicle runs on a 20-kilowatt-hour (kWh) lithium ion battery, allowing owners to charge the vehicle from a standard 110 volt, 10 amp outlet “overnight.”³ The vehicle’s seat fabric is made from recycled plastic bottles and as mentioned before, the vehicle’s internal temperature is controlled by a solar cell roof (Figure 2).

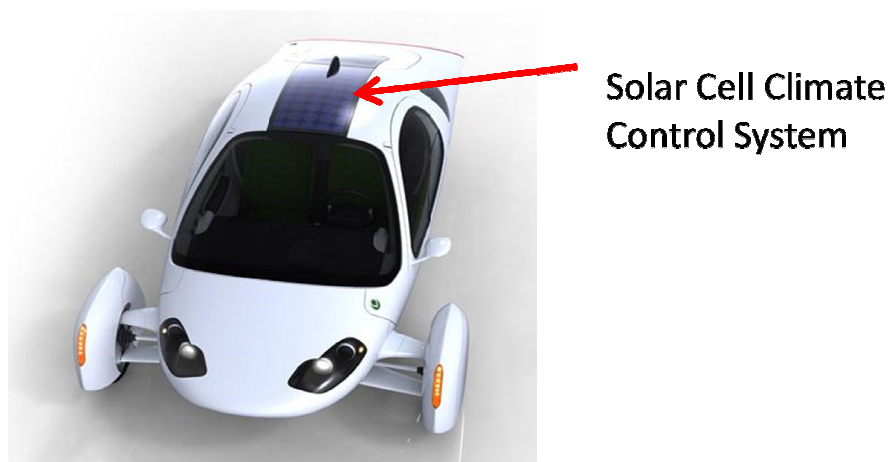


Figure 2: Top view of the Aptera 2e showcasing the solar cells on the roof of the vehicle that power the car’s climate control system.

The three wheel design of the vehicle over the more conventional four wheel design has been shown to reduce energy consumption by 35%¹. The use of a sandwich core composite in the car’s body, which is one quarter the density of steel, causes the vehicle to have a curb weight (total mass of the vehicle) of 816 kg. A combination of the vehicle’s weight and unique design has resulted in the vehicle using 80 Wh/mile at 55 mph. The EPA has estimated that the vehicle has a combined highway/city range of 100 miles, equating to 200 mpg efficiency using 2009 Californian residential electricity and gasoline rates⁴. It should be noted that although the Aptera 2e currently employs battery technology to power itself, Aptera has stated that their vehicle is power train indifferent. The fuel efficiency of the vehicle is mainly

derived from its shape, design, and material system, thus future iterations of the vehicle could be powered by a more traditional combustion engine or hybrid system.

1.2.2 Production of the 2e

As of June 2010 the car has not been put into production, although Aptera hopes to start production by fourth quarter 2010⁵. Currently, a \$500 fully refundable deposit can be made for a 2e through Aptera's website. Although Aptera has not identified a specific price point, current estimates have placed the price between \$20,000-40,000 depending on which additional features the buyer adds⁵.

The 2e has numerous environmental advantages over current automobiles, but the social ramifications of the car could be even greater. Substantial increases in fuel prices in the last decade have discouraged consumers from purchasing low efficiency sport utility vehicles (SUVs). SUVs have been the primary focus of the "Big Three" (Ford, General Motors, Chrysler) American automakers due to their high profit margins⁶. In 2008, the credit crunch experienced by the nation's financial industry put pressure on the price of raw materials and the availability of credit to consumers. These factors were largely responsible for a 26.6% drop in industry sales and forced America's major auto makers to experience record losses⁶. Acceptance of the vehicle has the possibility of helping restore America's auto industry by providing numerous domestic jobs within the United States and specifically in California, in which Aptera has pledged to have their production facilities¹. Aptera estimates that 2,500 jobs (500 within Aptera and 2,000 indirectly with their suppliers) will be created when the vehicle goes into production⁷.

1.2.3 Safety of the 2e

Because the vehicle only has three wheels, it is classified as a "motorcycle" by most states and is not required to follow mandatory safety or auto emission standards required of conventional automobiles. However, Aptera has made it a priority not to trade fuel efficiency for safety and has made it their mission to abide by all automotive standards. To ensure that the vehicle is safe for highway use, a finite element analysis (FEA) model has been created that simulates various impacts to the car's body to determine the vehicle's ability to protect its passengers⁷. The FEA model utilizes the vehicle's shape and design in conjunction with the mechanical properties of the composite material employed to simulate its impact resistance. The mechanical properties utilized in the model can be measured by various ASTM standards that have been approved by experts within the composites industry.

1.3 General Background on Polymer Matrix Composites

The 2e's body is made of a proprietary polymer matrix composite (PMC). This particular PMC consists of thin fiber reinforced composite sheets (face sheets) bonded to a thicker honeycomb core (Figure 3).

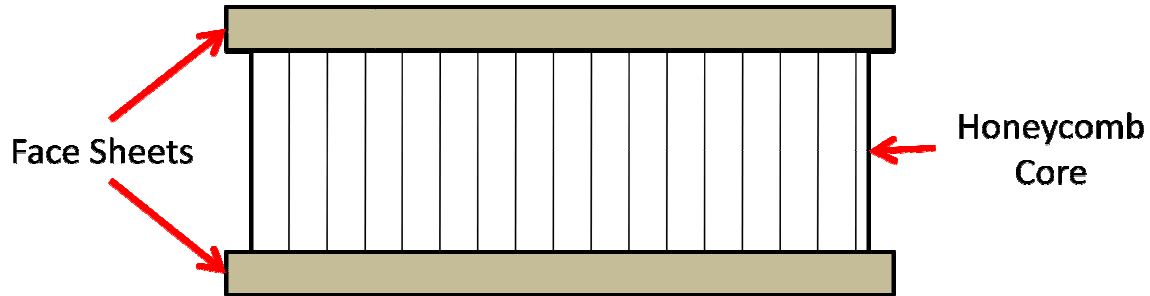


Figure 3: Schematic of a PMC showing the fiber reinforced face sheets “sandwiching” the honeycomb core.

The face sheets are composed of E-glass fibers of high strength and modulus embedded in an epoxy matrix. Within the face sheet, both the E-glass fiber and the epoxy matrix retain their physical and chemical identities; but produce a combination of properties that is superior to either of the individual constituents⁸. As result, fiber reinforced composites can be manufactured to produce strength values that are comparable to common structural engineering alloys such as 2024-T3 aluminum and AISI 1025 Steel (Table I).

Table I: Properties of Typical Fiber Reinforced Composite Materials and Structural Metals⁹

Material	Density (g/cm ³)	Tensile Strength (MPa)	Specific Strength (TS/ ρ)	Tensile Modulus (GPa)	Specific Modulus (E/ ρ)
AISI 1025 Steel	7.80	394	51	207	26.5
2024-T3 Al	2.80	414	148	79	28.2
E-glass/ Epoxy Fabric	1.90	433	228	24.5	12.9
Kevlar 49/Epoxy Fabric	1.38	369	267	29	20.7

What makes fiber-reinforced composites useful in many applications is the material’s low density which causes the composite to have high specific strength values compared to other structural materials. As a result, PMCs have replaced metals in various weight-critical components in aerospace, military, sporting goods, and automotive applications⁹.

Fiber reinforced composites exhibit high strength due to the fibers acting as the principal load carrying member. The surrounding epoxy matrix, which is sometimes referred to as the continuous phase, helps keeps the fibers in the desired orientation, acts as load transferring medium between individual groups of fibers, and provides shape and size stability for the material¹⁰. In addition, the epoxy matrix protects the fibers from environmental damage, thus allowing for their use in a variety of harsh environments⁸. Mechanical properties of the composite are highly influenced by the interface between the fibers and the matrix (known as the fiber-matrix interface). Surface defects on the fibers, inadequate wetting of the fibers, and pores at the fiber-matrix interface have been shown to decrease the strength and stiffness of the composite¹¹. To help improve the bonding between the fibers and the matrix, the fiber surfaces are often modified before they are surrounded by the continuous phase, a process known as *wetting*. E-glass fibers are particularly susceptible to surface defects when uncoated. To prevent this problem, manufacturers typically apply surface treatments or *sizing* in the form of an organic coating to protect the surface of the fibers from defects when being handled¹¹. Numerous studies have shown that applying a silane coating to E-glass fibers embedded in an epoxy matrix greatly improves the adhesion at the fiber-matrix interface⁸. Depending on fiber supplier's manufacturing process, different fibers of identical composition can produce large variation in properties because of these surface treatments and how the fibers are handled.

1.3.1 Applications of PMCs in the Transportation Industry

The aerospace industry has embraced PMCs mostly due to their high specific strength and modulus. PMCs are currently being employed in the fuselage of the Airbus A380 and the Boeing 787 "Dreamliner", in which composite materials account for 50% of the weight⁹. The Cobra tram in Zurich, Switzerland also utilizes a sandwich core composite to help reduce the weight of the train while making it stronger⁹. However, recent advances in fiber reinforced composites within the aerospace industry have not carried over to the automobile industry. According to Toyota, the following problems must be addressed before wide-scale adoption of composite materials can take place: obtaining a Class A surface finish (equivalent to the surface finish of steel panels), joining of composites, manufacturing, and cost². Although no major auto manufacturers have yet to release a commercially available fiber reinforced composite-based vehicle; some companies have developed concept cars based on PMC technology. One specific example is a General Motors concept car, the Ultralite, released in 1992. The Ultralite's body consisted of a carbon-fiber cloth over a PVC core, and was capable of achieving 88 mpg (Figure 4)⁵.



Figure 4: The Ultralite, a 1992 GM concept car, had a curb weight of 1400 lbs. The carbon-fiber body structure was built by Scaled Composites Co. and the vehicle contained a 1.5L, 111 hp engine⁵.

Positive response to the vehicle motivated GM engineers to conduct a study on production feasibility. Unfortunately, the slow cycle times to manufacture the composite structure's load-bearing panels would require multiple parallel manufacturing plants; that would result in a significant increase in the base cost of the vehicle and make it not viable for mass production⁵. Processing of PMCs requires labor intensive hand lay-up techniques which is adequate in production runs of less than a 1,000 components per year (aerospace components), but not as much for automotive applications that require production cycles of hundreds of components per day¹⁰. Currently, a typical auto plant can stamp out sheet metal parts at a rate of 60 jobs/minute, whereas it could take a couple of hours to cure a single fiber reinforced component of similar geometry¹². As a result, concerns with high manufacturing and raw material costs have steered major automakers away from incorporating composite materials into their vehicles.

However, within the automotive industry, niche applications of PMCs have made their way into body, chassis, and engine components⁸. For example, the Corvette's steel rear leaf spring was replaced with a composite leaf spring consisting of glass fibers embedded in an epoxy matrix that weighed a fifth of the previous steel spring⁹. Sheet modeled composites have also been used in non-primary structural applications such as body panels and pick-up truck boxes¹². In addition, a majority of PMC automotive components are making their way into vehicles in the form of after-market hoods, door panels, and fenders. Recently, the Japanese government invested billions of Yen into developing processes that would be able to mass produce cost effective, recyclable fiber reinforced composites with the goal to reduce vehicle mass by 40%⁵. Recent legislation passed by the US government that tightens emission

standards as well as increases the mandatory efficiency of vehicles (35 mpg by 2020) has started to force automobile manufacturers to reconsider the use of fiber matrix composites¹³.

Although a number of new techniques have been developed to help increase production efficiency, specifically vacuum bag molding, pressure bag molding, compression molding and autoclave molding; production costs are still preventing wide scale acceptance of PMCs in the automotive industry.

1.4 Manufacturing of Polymer Matrix Composites

Manufacturing of PMCs consists of incorporating large numbers of fibers into a polymeric matrix to form thin sheets. Each individual sheet is called a *lamina* or *ply*. In the case of continuous fibers, the fibers are typically arranged in bundles, called *tows*, in a unidirectional or bi-directional orientation to form a fabric. The fibers within a fabric remain in the correct orientation due to a weaving or stitching process employed by the fabric supplier⁸. Laminas typically have thickness between 0.1-1 mm and are stacked in a specific sequence, called a *laminate*, to obtain a desired thickness for a given load or deflection. When creating a laminate, the orientation of the fibers is critical in determining how the material reacts to different principal loads. Engineering alloys and most polymers typically exhibit isotropic behavior; material properties are the same in all direction. On the other hand, fiber-reinforced composites exhibit anisotropic behavior, which causes different material properties depending on the direction of fibers in the composite lamina or laminate. These properties can also be varied by the orientations of the fibers in a laminate called the *fiber orientation angle* (θ), which is used to describe the angle between a principal fiber direction and the other fibers in the laminate.

1.4.1 Aptera 2e's PMC Structure

Currently, the 2e's face sheets are made of Vectorply's (a company that manufactures and distributes composite reinforcement fabrics) quadraxial quasi-isotropic preformed fabric embedded in an epoxy matrix. Quasi-isotropic laminates are a unique type of fiber reinforced composite because they exhibit in-plane isotropic elastic behavior. However, strength properties may still vary with direction of loading⁷. Aptera's sandwich core composite utilizes two versions of Vectorply's preform fabrics, the E-QX 2600 and E-QX 3600 (the QX refers to the quadraxial structure, the E to E-glass, and the 2600/3600 to the amount of E-glass fiber present in the laminate). Both the preforms consist of four unidirectional E-glass fiber layers stacked on top of each other varying by 45° [0°, +45°, 90°, -45°]. The layers utilize Vectorply's "tricot" polyester stitching technique to ensure that the fiber orientation relative to each other remains constant (Figure 5)¹⁴. The E-glass fibers used within Vectorply's fabric consist of PPG's (a fiber glass

reinforcement manufacturer) *Hybon 2022* fibers. The 2022 fibers have a 24 μm diameter and utilize a silane sizing to protect the fiber surface and increase adhesion at the fiber-matrix interface¹⁵.

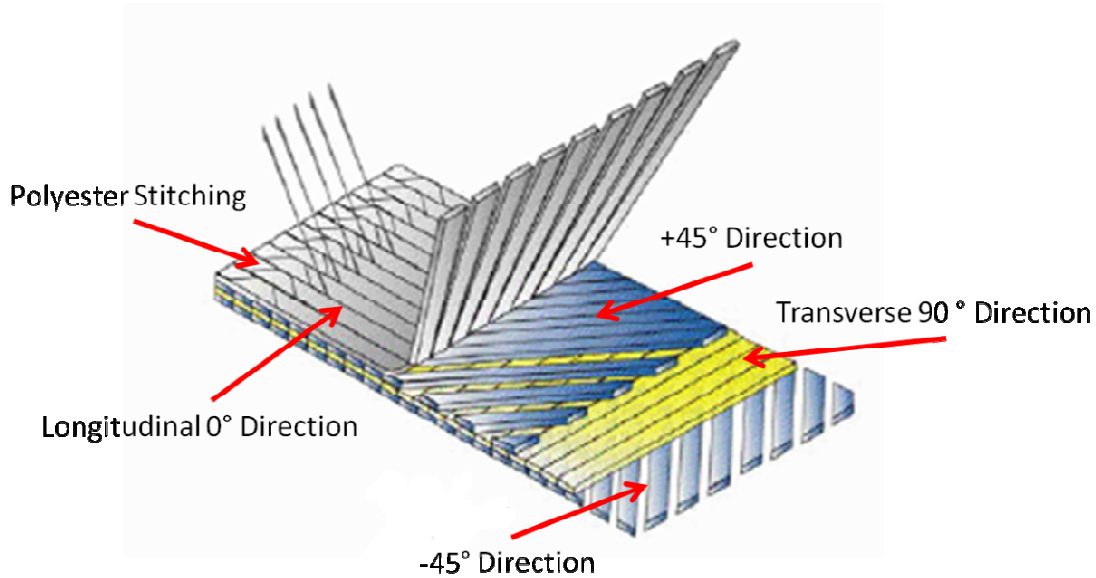


Figure 5: Schematic of Vectorply's preform fabric utilized in Aptera's fiber reinforced face sheets¹⁴.

The face sheet that would be present on the exterior of the vehicle is made of the E-QX 3600 preform, known as the *A surface*; the face sheet that would be seen from the interior of the vehicle consists of the E-QX 2600 fabric, known as the *B surface*. The two fabrics are identical in structure, but differ in the amount of E-glass fiber contained within each layer (Table II).

Table II: E-Glass Fiber Content in Vectorply's E-QX 2600 and E-QX 3600 Fabrics¹⁴

Fabric Type	Dry Thickness (mm)	0° Architecture (g/m ²)	-45° Architecture (g/m ²)	+45° Architecture (g/m ²)	90° Architecture (g/m ²)
E-QX 2600	0.95	217	212.5	212.5	211.5
E-QX 3600	1.30	303.7			

These fabrics are bonded to a honeycomb core to make up the vehicle's composite. Aptera's sandwich core composite currently uses Lantor's (a company that manufactures flexible nonwoven core materials for use in composites) *XF6 Soric* core. The XF6 core consists of a polyester nonwoven material with a compression resistant hexagonal (honeycomb) cell structure. The compression resistant cells are separated from each other by channels which help facilitate the flow of resin throughout the sandwich

core composite, but prevent the uptake of resin within the cell structure¹⁶. The resin flow channels cause the resulting PMC to have adequate mechanical properties and excellent adhesion between the core and its face sheets. The XF6 version of Lantor's cores is known for its fast resin flow and low resin consumption, thus making it ideal for thicker laminates (Figure 6)¹⁶.

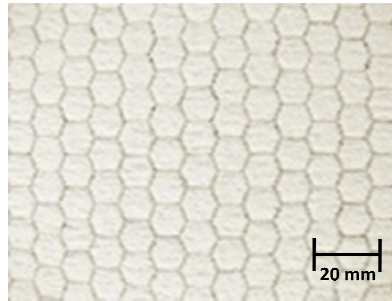


Figure 6: Lantor's Soric XF6 core which consists of a polyester hexagonal core structure separated by resin flow channels to allow for a homogenous dispersion of resin during the fabrication of a sandwich core composite.

Aptera utilizes a vacuum-assisted resin transfer molding technique to fabricate their sandwich core composites. In this fabrication method, a dry E-glass fiber reinforcement assembly is placed in a mold and then is injected with a mixture of resin and hardener. After the resin and hardener mixture have filled the mold, a prescribed time-temperature curing cycle is used to harden and dry the resin around the fiber fabrics to create the PMC⁹. In the 2e's PMC, Vectorply's E-QX 3600 fabric is placed on top of a protective veil (a fabric made from polyester that acts as a sponge during the resin injection process to improve the surface finish). The veil rests on an open mold surface while the honeycomb core is sandwiched between the E-QX 3600 and E-QX 2600 fabrics. The stack of materials is then covered with a vacuum bag which is sealed to the mold periphery (Figure 7).

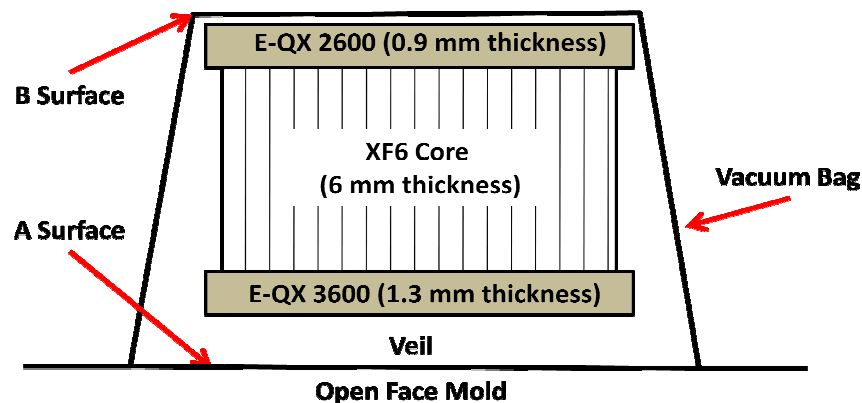


Figure 7: Stacking sequence of Aptera's sandwich core composite within the vacuum-assisted resin transfer mold.

After the vacuum bag is secured over the PMC's constituents, resin is injected into one point of the vacuum bag, while a vacuum is drawn from another point. The resin flow is assisted by the vacuum to ensure a homogenous coating of the resin on the E-glass fabrics. The composite is then cured for a set time and temperature within the mold. The composite is then removed from the vacuum bag and undergoes a post cure cycle for two hours at 140°F and another two hours at 185°F⁷. This manufacturing technique requires less expensive tooling than other composite manufacturing processes, but only allows for one side of the composite to be against the mold face⁹, in this case the E-QX 3600 face sheet. Having the face sheet next to the mold face produces a smoother surface finish than the face sheet in direct contact with the vacuum bag. However, since the A surface is the only visible surface this disadvantage is not a major concern for Aptera.

1.5 Project Objectives

Aptera in partnership with a third party company has created an FEA model that simulates various loading conditions that the cabin of the vehicle could be subjected to in an accident. The FEA model utilizes specific mechanical properties of the vehicle's composite body which can be experimentally determined through mechanical testing following specific ASTM standards. The properties required for the FEA model and their appropriate ASTM standards are summarized in Table III.

Table III: Mechanical Properties Required for the Aptera 2e FEA Model

Material Property	ASTM Standard	Laminate Structure
Tensile Strength	D3039	[0°, +45°, 90°, -45°]
Tensile Modulus		
Compressive Strength	D695	[0°, +45°, 90°, -45°]
In-plane Shear Strength	D3518	[+45°, -45°]
In-plane Shear Modulus		
Short Beam Strength	D2344	[0°, +45°, 90°, -45°]
Core Shear Modulus	D7250	[0°, +45°, 90°, -45°] + Core material
Core Shear Strength	C393	

The purpose of the project was to validate a secondary fabric supplier, Saertex, as well as characterize two alternate core materials (Lantor's TF2 and LRC3 cores) for use in future iterations of Aptera's PMC. Validation was accomplished by experimentally determining the density, surface finish, tensile modulus

and strength, in-plane shear modulus and strength, compressive strength, and short beam strength of laminates containing Saertex's fabrics. The mechanical properties of the alternate supplier's fabrics were then compared to Aptera's current fabric to determine if they are adequate for use in their PMC. Characterization of the alternate cores was done by experimentally determining the core shear strength and modulus, density, and surface finish of two alternate cores. However, due to equipment constraints at Cal Poly, the in-plane shear modulus, surface finish, and compressive strength of Saertex's fabrics could not be characterized. In addition, the core shear modulus of the alternate cores could not be characterized. As an alternative, the flexural modulus was characterized for the cores instead of the core shear modulus.

Aptera believes that having a secondary supplier for the majority of their components is critical in maintaining a strong supply chain⁷. If their current fabric supplier became backordered, raised prices, or went out of business, Aptera could switch over to the alternate fabric supplier without a significant loss of production. In addition, if the alternate core materials exhibited an increase in core shear properties or a decrease in density it could cause Aptera to select one of the alternate cores in a future generation of the 2e, thus leading to a lighter weight and more fuel efficient vehicle⁷.

1.5.1 Saertex Fabric

The secondary fabric supplier that was validated in this project was Saertex (a fabric supplier that is known for their non-crimp fabrics). The Saertex fabric is similar to the Vectorply fabric in that it consists of 36 oz. of E-glass fiber in a stitched quadraxial layup. Saertex also utilizes a non-crimp stitching technique in their fabrics. Saertex's fabrics consist of PPG's *Hybon 2026* E-glass fibers, a newer version of PPG's *Hybon 2022* fibers used within Vectorply's fabrics¹⁷. The *2026* fibers have a similar 24 μm diameter, but utilize a different silane sizing which PPG claims increases wetting of the fibers¹⁸.

1.5.2 Alternate Core Materials

The two alternate core materials characterized in this project were Lantor's LRC3 and TF2 cores. The LRC3 core is similar to the XF6 core in that it consists of a polyester compression resistant hexagonal cell structure separated by resin flow channels. However, the LRC series is known for its low resin consumption which is due to larger honeycomb cells resulting in less resin flow channels per surface area. This results in a less dense composite compared to Lantor's other cores (Figure 8).

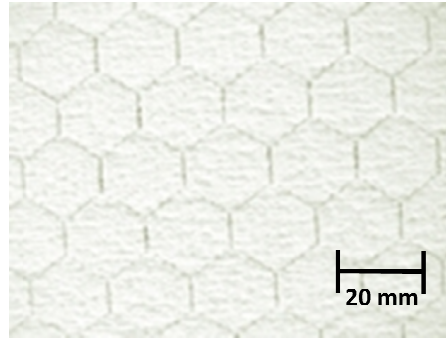


Figure 8: Photograph of Lantor's Soric LRC core material. The honeycomb cell structure is 4.3x larger than XF6's structure causing the composite to uptake less resin during the resin infusion process.

In addition, the LRC3 core is only 3 mm in thickness, thus to obtain the same thickness as the XF6 core two of the core materials were stacked directly on top of each other and sandwiched by two facesheets containing Vectorply's fabrics.

The other core material that was characterized in this study was Lantor's Soric TF2 core. The TF2 core consists of a polyester nonwoven dot-printed cell structure. The TF series is known for the high quality surface finish the core creates in the finished sandwich core composite. This is due to the core eliminating impressions created by the honeycomb structure during the vacuum infusion process (Figure 9).

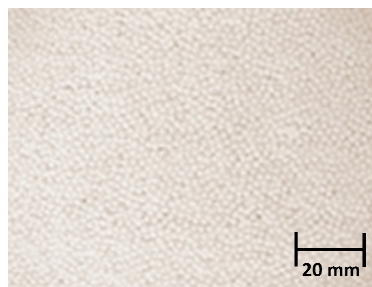


Figure 9: Lantor's Soric TF core that consists of a dot-printed cell structure. This core is typically paired with another core material to achieve adequate core properties¹⁶.

Similar to the LRC3 core, the TF2 core is not as thick as the XF6 core material. To achieve the same thickness as the XF6 core, the TF2 core (2 mm thick) was stacked on top of an LRC4 core (4 mm thick). The LRC4 core is identical to the LRC3 core except for the thickness. In the completed sandwich composite, the TF core was situated on the A surface to allow for a better surface finish. Like the other two cores, the TF2/LRC4 combo was sandwiched between two facesheets containing Vectorply fabrics.

2. Experimental Procedures

This section contains the experimental procedures used to measure the mechanical properties of laminates containing Saertex fabrics as well as the procedures used to characterize the core shear properties of the alternate cores.

2.1 Experimental Procedure used in the Validation of Saertex Fabrics

The Instron 3369 testing system running Bluehill v.1.5 software was used to determine the mechanical properties of face sheets containing Aptera's current fabric (Vectorply) and alternate fabric (Saertex). All laminates tested were fabricated by Aptera utilizing their vacuum-assisted resin transfer technique. The laminates were fabricated into 20"x 20" panels and then machined to their appropriate length and width for test samples. The samples then underwent a post-cure at 140° F for two hours followed by an additional two hours at 185° F. All samples were tested following the appropriate ASTM standard. For each test procedure, sample width and thickness measurements were made in three locations before performing the test.

2.1.1 Determination of In-plane Tensile Strength and Modulus

To determine the tensile strength and modulus of the face sheets, uniaxial tensile tests were performed following ASTM D3039¹⁹. Each sample consisted of two 36 oz. fabrics embedded in an epoxy matrix. Following ASTM D3039's recommended specimen geometry, samples were machined to have a nominal 25 mm width and 150 mm length rectangular cross-section. Preliminary testing of samples of this geometry exhibited failure within the gage length without the use of *tabs* (additional material bonded to the end of a tensile sample to prevent slippage between the grip face and the test coupon).

Specimens were loaded in the Instron so that the length was aligned with the test direction and the grips were hand tight. An Epsilon 3542-025M-ST extensometer (25 mm gage length) was secured to the sample to monitor the beginning strain response. Each sample was monotonically loaded at a constant crosshead displacement rate of 2.00 mm/minute until failure. During the test, force versus crosshead displacement data and force versus strain data were recorded every 330 milliseconds; however, the extensometer was removed from the sample at 5% strain in order to protect the equipment. After the test, the location and type of failure was recorded using ASTM D3039's three-part failure mode code.

Ultimate tensile strength (F^u) was determined by the maximum force (P^{\max}) carried by the sample before failure (Eq. 1). The tensile modulus of elasticity (E^{chord}) was calculated by taking the slope of the stress-strain plot at 1000 and 3000 $\mu\epsilon$ strain (Eq. 2)¹⁹.

$$\mu_{tu} = \frac{P^{max}}{A} \quad (1)$$

$$E_{chord} = \frac{\Delta\sigma}{\Delta\epsilon} \quad (2)$$

Within the equations, A is the nominal cross-sectional area, $\Delta\sigma$ is the difference in applied tensile stress at 1000 and 3000 $\mu\epsilon$ strain, and $\Delta\epsilon$ is the difference in strain which remained constant at 2000 $\mu\epsilon$.

2.1.2 Determination of In-plane Shear Strength

Petit and Rosen²⁰ proposed that the in-plane shear response of a laminate can be determined by a similar method as the in-plane tensile response except that a $\pm 45^\circ$ laminate must be used. Through lamination theory, they showed that a state of shear stress (τ_{12}) in the lamina coordinate system (1,2 directions) can be expressed in terms of the laminate axial stress (σ_1) (Eq. 3).

$$\tau_{12} = \frac{\sigma_1}{2} \quad (3)$$

To determine the laminate axial stress, uniaxial tensile tests were performed following ASTM D3518²¹. Two different sample thicknesses were fabricated by Aptera. Initially the samples consisted of two $\pm 45^\circ$ fabrics adhered together. However, testing on samples of this geometry experienced bowing when the extensometer was attached. Subsequent samples were composed of eight $\pm 45^\circ$ fabrics to prevent bowing. As the fabrics were stacked on top of each other careful attention was made to ensure that the fabric's fibers were aligned with each other ($\pm 45^\circ$). Each sample was then machined to have a rectangular cross-section with a width of 25 mm and a length of 150 mm in accordance with ASTM D3039, while taking care to ensure that the fibers were 45° to the length of the sample (Figure 10).

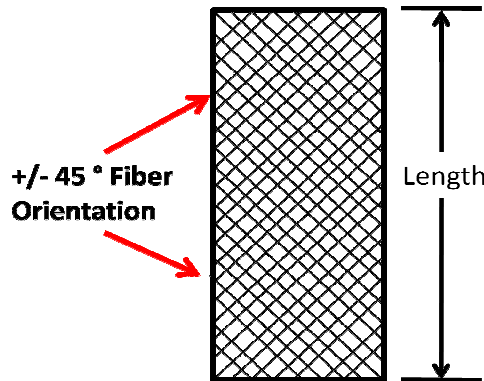


Figure 10: Schematic of an in-plane shear sample showing the fibers orientated $\pm 45^\circ$ to the length of the sample.

The samples were secured in the grips of the Instron and the same Epsilon extensometer was attached to the sample to monitor the longitudinal strain response. Each sample was monotonically loaded at a constant crosshead displacement rate of 2.00 mm/min until 5% longitudinal strain. The principal reason for terminating the test at 5% strain is due to the occurrence of extreme fiber scissoring in samples of this geometry. Kellas et al, estimated that the fibers rotate approximately 1° for every 2% of axial strain²¹. Such fiber scissoring would cause a violation of the assumption that test is of a nominal +/- 45° laminate if continued past 5% shear strain.

According to ASTM D3518, the maximum in-plane shear strength (τ_{12}) of the laminate is calculated by the maximum load experienced by the sample at or below 5% shear strain. However, due to equipment constraints, the lateral normal strain could not be measured and thus the shear strain could not be computed for the tests. As a substitute, the maximum load at 5% longitudinal normal strain was used instead (Eq. 4).

$$\tau_{12} = \frac{P^m}{2A} \quad (4)$$

In equation 4, P^m is the maximum load at or below 5% longitudinal strain and A is the cross-sectional area. The maximum in-plane shear strength calculated by this procedure is a conservative estimate. Since shear strain is found by subtracting the lateral strain from the longitudinal strain, the extension of the sample at 5% longitudinal strain will always be less than that at 5% shear strain in materials that exhibit a positive Poisson's ratio.

2.1.3 Determination of Short-Beam Strength

The short-beam strength was determined by subjecting a laminate to three-point bending following ASTM D2344²². The short-beam strength is used as a substitute for characterizing the interlaminar shear strength of a composite laminate. The short-beam samples consisted of six layers of 36 oz. E-glass fiber fabrics embedded in an epoxy matrix. According to the standard, the geometry of the specimens should conform to the following guidelines:

$$\text{Specimen length} = \text{thickness} \times 6.0$$

$$\text{Specimen width} = \text{thickness} \times 2.0$$

To perform the test, the samples were inserted into a 3-point bend test fixture so that the specimen's longitudinal axis was perpendicular to the loading nose and side supports. The support span length of

the sample was adjusted to create a span-to-measured thickness ratio of 4.0 and the loading nose was positioned equidistant between the side supports²² (Figure 11).

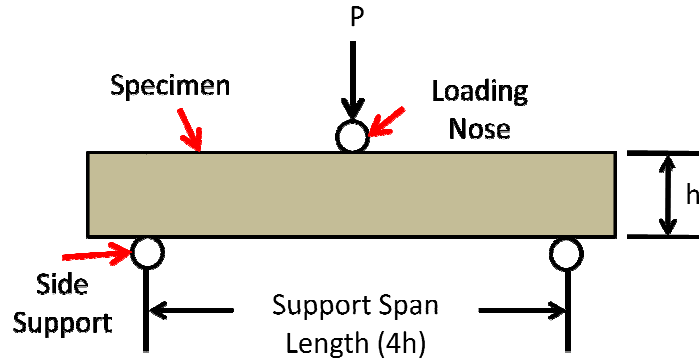


Figure 11: Schematic side view of a short-beam strength sample loaded in a 3-point bend test fixture. The span length is a function of the thickness (h).

Each sample was loaded at a constant crosshead displacement rate of 1.0 mm/min until a sharp load drop-off of 30%. A variety of failure modes (interlaminar shear, flexure, or inelastic deformation) can occur when using this method; however, failures are typically a result of resin and interlaminar properties. The short-beam strength (F^{sbs}) was calculated using the following equation (Eq. 5):

$$F^{sbs} = 0.75 \times \frac{P_m}{b \times h} \quad (5)$$

In this equation, P_m is the maximum load experienced by the specimen before failure, b is the measured specimen width, and h is the measured specimen thickness. Since multiple failure modes are possible, this method is generally used as a comparative test between composite materials of the same geometry and stacking sequence that fail in a consistent mode²².

2.2 Characterization of Alternate Core Materials

Flexure tests on a flat sandwich composite were used to determine the core shear strength and flexural modulus of the various cores. A three-point bending configuration was used to apply a load on the specimen in such a manner that the applied moments cause the sandwich face sheets to bend²³. The cores were bonded to two face sheets containing Vectorply's fabric to form a sandwich core composite. Specimens were machined and fabricated by Aptera using their vacuum-assisted resin transfer technique. Specimen geometry followed recommendations outlined in ASTM C393²³ resulting in a nominal width of 40 mm and a nominal length of 200 mm.

The samples were subjected to a compressive load in three-point bending at a constant crosshead displacement rate of 2.00 mm/min until failure. The support span length was set to 150 mm as recommended by ASTM C393 for specimens of this geometry. An Epsilon 3540-006M-ST deflectometer (6.00 mm range) was positioned beneath the sample directly under the fixture's loading nose to monitor the beam's deflection during the test. The deflectometer was removed after 4 mm deflection to protect it from being damaged. After the test, the mode, area, and location of the failure were recorded using ASTM C393's three part failure code.

2.2.1 Determination of the Core Shear Strength

The core shear strength was calculated from the maximum force (P_{max}) the specimen experience prior to failure (Eq. 6).

$$F_s^{ult} = \frac{P_{max}}{(d + c)b} \quad (6)$$

In equation 6, b is the measured specimen width, d is the measured sandwich thickness, and c is the core thickness (Figure 12).

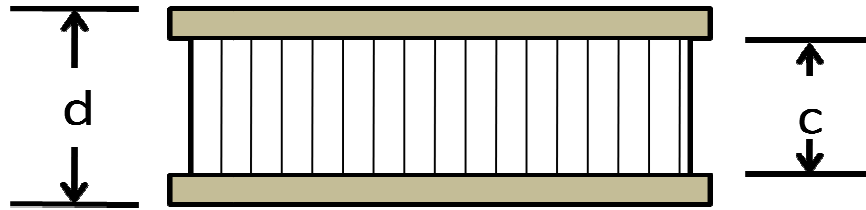


Figure 12: Schematic of a core shear sample showing the core thickness and the sandwich thickness. The width of the sample (b) would be going into the page.

Since it is difficult to accurately measure the core thickness after the face sheets have been bonded to the core, the core thickness was instead calculated by subtracting nominal facing thicknesses (estimated by Aptera to be 1.00 mm) from the measured sandwich thickness (d) (Eq. 7).

$$c = (d - (2t)) \quad (7)$$

2.2.2 Determination of Flexural Modulus

Initially, ASTM C393 in conjunction with ASTM 7250²⁴ was used to determine the core shear modulus of the alternate cores. However, the equations outlined in the ASTM 7250 were unsuccessful in calculating

sensible values and instead the flexural modulus was used as a substitute to quantitatively compare the modulus of the cores in bending.

To determine the flexural modulus (E^f) of the specimen, the force vs. deflection data from the core shear strength test was used. The flexural modulus was calculated by the following equation (Eq. 8):

$$E^f = \frac{ML^3}{4wh^3} \quad (8)$$

Where M is the slope of the first linear region on a force vs. deflection curve, L is the support span length (150 mm), w is the measured specimen width, and h is the measured specimen thickness. The first linear region on the force vs. deflection curve was determined to be within the first 2.5 mm of deflection. As a result, a two point analysis was used to calculate the slope by taking the difference in load between 1.00 mm and 2.00 mm deflection (Figure 13).

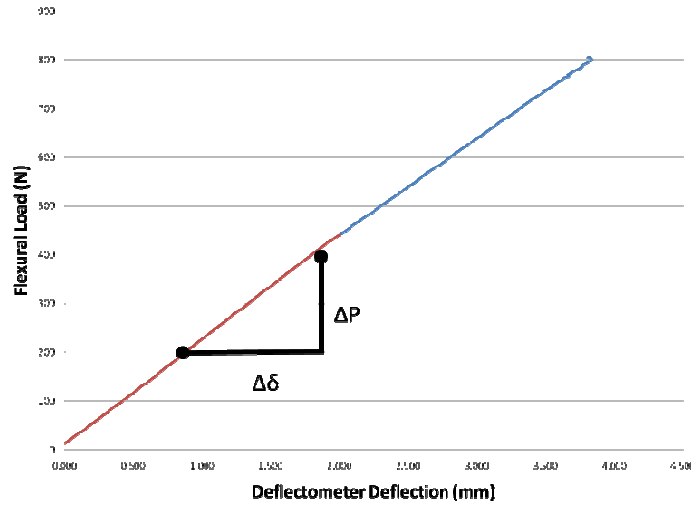


Figure 13: Representation of how the slope of the first linear region was calculated using points at 1.00 and 2.00 mm deflection.

The initial linear region's slope was also calculated by performing a linear regression between 0 mm and 3 mm deflection. The linear regression method showed that the slope was linear ($R^2 = 0.9989$) and was producing values that were within 5% of those determined by the two-point method.

2.3 Scanning Electron Microscopy

Scanning electron microscopy was used to examine the fracture surfaces of the uniaxial tensile test specimens. Fiber pull-out and fiber fracture surfaces of samples from both fabric suppliers were

examined in an attempt to qualitatively compare the adhesion of the matrix to the fibers. The samples were examined using an FEI Quanta 200 SEM in secondary electron imaging mode at high vacuum (5×10^{-5} torr) and an excitation voltage of 2 keV. To help prevent charging of the samples, copper tape was attached to the specimen and a metallic sample mount. This technique did not fully prevent charging of the sample, but did allow for an adequate amount of time to capture images. Other techniques were attempted to reduce charging such as sputtering the sample with a thin gold film and imaging the sample at low vacuum while introducing water vapor into the chamber. However, due to equipment issues neither of these techniques was successful.

3. Results and Statistical Analysis

This section contains the results obtained from the experimental testing of the two fabric suppliers and the three core materials. A two-sample t-test was utilized to determine if the average mechanical properties exhibited by the two fabric suppliers and the three cores were statistically different from one another. When using a two-sample t-test, the two random samples must be selected independently and come from normal populations. In addition, for the t-test to be valid each experimental test's sample population must exhibit a Gaussian distribution which was tested for by using the Anderson-Darling normality test²⁵. The null hypothesis for each test was set at 0 ($\Delta = 0$) and alpha value of 0.05 was used to determine if the means were statistically different.

3.1 Results of Secondary Fabric Validation

It was found that Saertex was superior to Vectorply in all mechanical properties tested. To determine the magnitude at which Saertex outperformed Vectorply, a 95% confidence interval was generated to quantify the difference in the means of each property.

3.1.1 Tensile Test Results

Ten preliminary tensile tests conducted on the Vectorply samples exhibited a tensile strength and modulus that was similar to baseline results that Aptera had already obtained; therefore it was deemed that the Instron was accurately measuring the tensile strength and modulus. Twenty-three samples containing Vectorply's fabric and twenty samples containing Saertex's fabric were then tested until failure. All samples tested failed in an explosive manner and the mean tensile strength and modulus was calculated for each supplier (Figures 14 & 15).

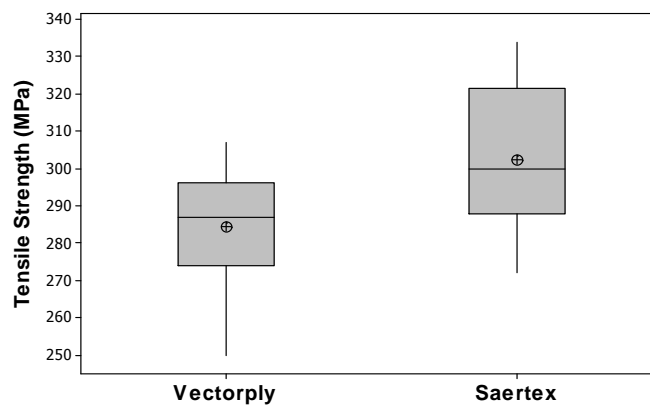


Figure 14: Graphical comparison of the two fabric supplier's tensile strength. The mean tensile strength of each supplier is indicated by the cross-hair mark on the graph.

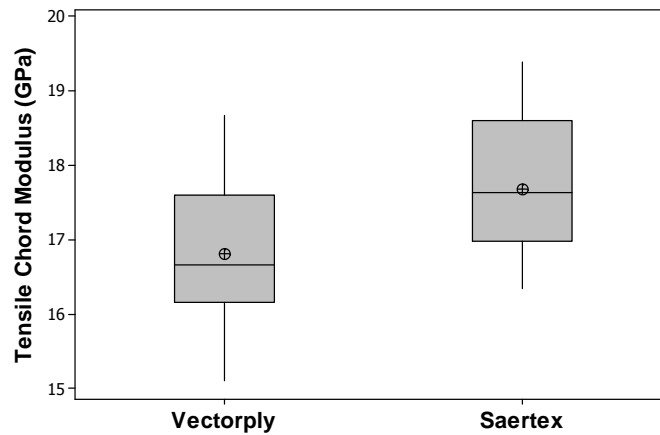


Figure 15: Statistical boxplot comparing the variation in the tensile modulus of the two fabric suppliers. The mean tensile modulus is identified by the cross-hair mark on the plot.

Between the two fabric suppliers, only one sample from each supplier failed within the grip section; both of these samples were disregarded when calculating the mean tensile strength. For the tensile strength data, both sample sets passed the Anderson-Darling normality test at an α value of 0.1 (p-value = 0.15 and 0.27, respectively). The two-sample t-test confirmed that the tensile strength of the two fabric suppliers was statistically different (p-value= 0.002). Laminates containing Saertex's fabric had a greater mean tensile strength than laminates containing Vectorply's fabric (95% CI: 6.7-28.9 MPa). The results of the tensile test are summarized in Table IV.

Table IV: Summary of Laminate Tensile Test Results

Fabric Supplier	Vectorply Fabrics	Saertex Fabrics	Difference in Means ($\mu_{\text{Saertex}} - \mu_{\text{Vectorply}}$)
Mean Tensile Strength (MPa)	285	302	6.7 - 28.9
StDev of TS (MPa)	16	20	-
Tensile Modulus (GPa)	16.8	17.7	0.29 – 1.47
StDev of E (GPa)	0.94	0.92	-

As with the tensile strength data, both tensile modulus data sets passed the Anderson-Darling normality test (p-value = 0.51 for both) and were statistically different from one another (p-value = 0.004). Using a 95% confidence interval, Saertex's fabric was found to have a mean tensile modulus that exceeded Vectorply's fabric by 0.29-1.47 GPa.

3.1.2 Short-Beam Strength Results

Similar to the tensile tests, preliminary tests were conducted on samples containing Vectorply's fabric and compared to Aptera's baseline database to ensure accurate measuring. The preliminary samples exhibited a mean short-beam strength that was within 10% of Aptera's baseline value and thus the test was deemed accurate. Thirty samples from each supplier were tested until failure. All samples failed due to interlaminar shear (Figure 16) and the mean short-beam strength was calculated for both suppliers (Figure 17).

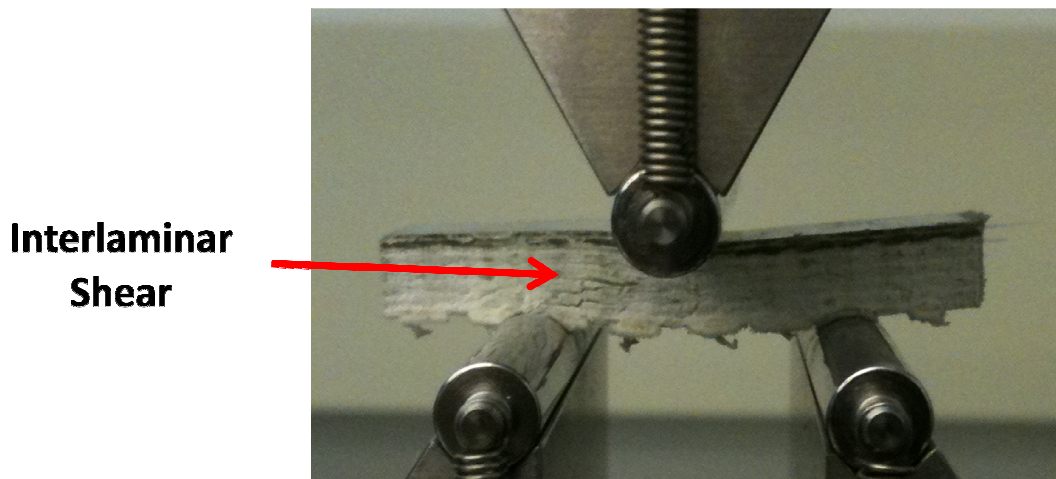


Figure 16: Failed Vectorply short-beam strength sample due to interlaminar shear shown by the red arrow.

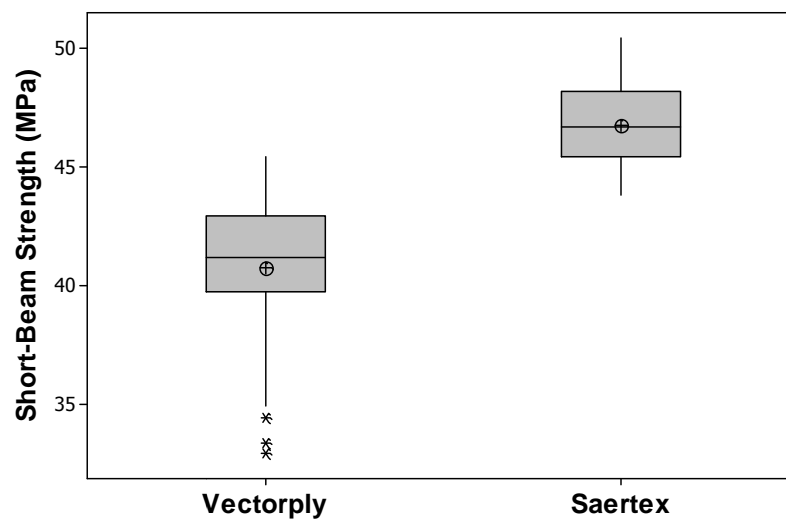


Figure 17: Statistical comparison of Vectorply and Saertex's short-beam strength. The mean is denoted by the cross-hair symbol while outliers are denoted with an asterisk.

The mean short-beam strength for Vectorply and Saertex was determined to be 40.8 and 46.8 MPa with standard deviations of 3.3 and 1.7 MPa, respectively. The boxplot showed that the Vectorply sample set contained three outliers which caused the Anderson-Darling normality test to fail (p -value < 0.005). However, when the outliers were removed, the sample set passed the Anderson-Darling normality test (p -value = 0.55); Saertex also passed the normality test (p -value = 0.43). In order to compare the two sample sets with a two-sample t-test the data sets must have a normal distribution, thus the outliers were omitted from the statistical analysis. Without the outliers, Vectorply exhibited a mean short-beam strength of 41.8 MPa with a standard deviation of 1.88 MPa. Even with the outliers excluded, the two fabric suppliers' short-beam strengths were still statistically different (p -value < 0.001). Saertex had a mean short-beam strength that was 3.97-5.88 MPa greater than Vectorply (95% confidence interval).

3.1.3 In-Plane Shear Strength Results

Testing was first conducted on laminates containing Vectorply's fabric that consisted of two $\pm 45^\circ$ biaxial fabric weaves adhered together. Preliminary tests of the Vectorply fabrics exhibited in-plane shear strength results similar to that of Aptera's baseline value (within 10%). However, when the extensometer was placed on the sample, the samples exhibited some amount of bowing. To prevent future bowing, the Saertex samples were requested to be made thicker and instead consisted of eight layers of $\pm 45^\circ$ biaxial fabric, with the assumption that a 4x increase in thickness should result in a proportional increase in load. However, during testing, the thicker Saertex samples exhibited an approximate 8x increase in load at 5% strain compared to the original Vectorply testing (Figure 18).

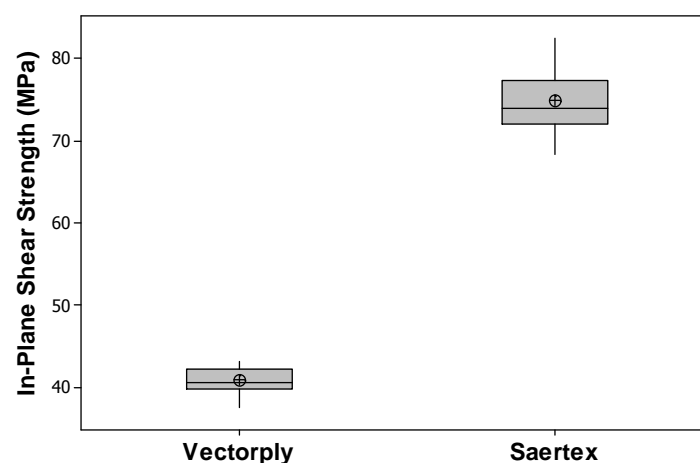


Figure 18: Boxplot comparing the in-plane shear strength of the two fabric suppliers. The Saertex fabrics exhibited shear strengths that were nearly two times that of Vectorply.

Vectorply exhibited a mean in-plane shear strength of 40.88 MPa with a standard deviation of 1.61 MPa. On the other hand, Saertex exhibited a mean in-plane shear strength of 74.95 MPa an 80% increase compared to Vectorply with a standard deviation of 3.79 MPa. Both sample sets passed the Anderson-Darling normality test (p-value =0.89 and 0.43, respectively). If the other tests were an indication, a small increase in in-plane shear strength was to be expected, however an increase of 80% might suggest that external factors beside the fabric supplier were occurring. The Saertex samples were made 10 mm wider than the Vectorply samples and a portion of the width protruded from the tensile grips. To ensure that the protrusion from the grips was not the cause for the increase in in-plane shear strength, three of the samples were cut to a nominal width of 25 mm (the same width as the Vectorply samples). The Saertex samples with the reduced width exhibited the same in-plane shear strength as the other Saertex specimens. With that in mind, the two-sample t-test confirmed that the two means were statistically different and the Saertex fabrics exhibited a mean in-plane shear strength that was 32.1-36.0 MPa greater than Vectorply's in-plane shear strength (95% confidence interval).

3.1.4 Laminate Density Calculations

The mass per surface area was found for each fabric supplier by measuring the width and length of two tensile samples and dividing it by the total mass of the sample. The resulting mass per surface area, in addition to the specific strength and modulus is presented in Table V.

Table V: Mass per Surface Area and Specific Mechanical Properties of the Two Fabric Suppliers

Fabric Supplier	Mass/surface area (g/cm²)	Specific Strength (MPa/ (g/cm²))	Specific Modulus (GPa/ (g/cm²))	Total Mass Savings (kg)
Vectorply	0.360	792	46.7	-
Saertex	0.344	878	51.5	6.3

The total mass saving is the change in mass of the vehicle if Saertex fabrics were used instead of Vectorply. The calculation was done by taking the calculated density and multiplying it by the total surface area (37.16 m² or 400 ft²) of composite material contained within the vehicle's body. It should be noted that the density calculation does not take into account the thickness of the sample which was shown to vary by 0.3 mm in the tensile samples. These values should be only used for a preliminary comparison due to the small sample set and variability in the thickness of the samples measured.

3.2 Results of Alternate Core Characterization

To determine the core shear strength and flexural modulus, twenty flexural tests were conducted on flat sandwich composites for each core. Similar to the fabric validation, a two-sample t-test was used to compare the mean core shear strength and mean flexural modulus of the two alternate cores (TF2 and LRC3) to Aptera's current core (XF6). When a statistical difference between the means existed, a 95% confidence interval was generated to determine the magnitude of the difference.

3.2.1 Core Shear Strength Results

Preliminary testing of samples containing Aptera's current core material, XF6, were conducted first and compared to Aptera's baseline database to determine if the test method and equipment was accurately measuring the core shear strength. The preliminary results showed that the test method was measuring a core shear strength that was within 5% of Aptera's baseline value. The remaining XF6 and the two alternate core samples were then tested until failure. After each test, the failure mode of the sample was recorded and the mean core shear strength was calculated (Figure 19).

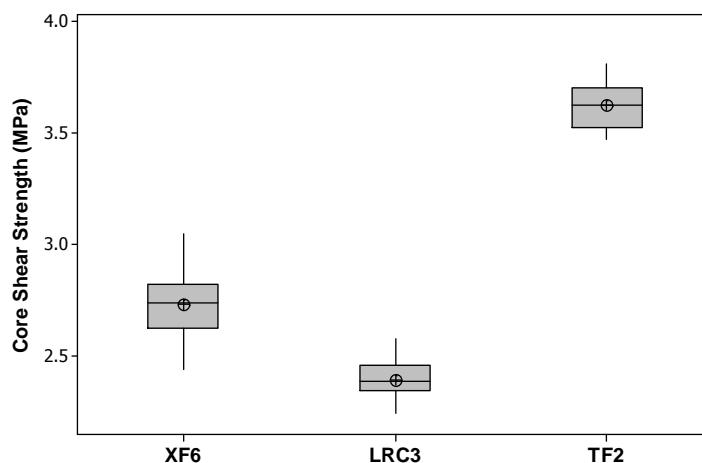


Figure 19: Boxplot comparing the core shear strength of the three core materials. Some samples of the LRC3 and TF2 cores were excluded from the boxplot due to unacceptable failure modes.

The XF6 core exhibited a mean core shear strength of 2.73 MPa and a standard deviation of 0.2 MPa; comparatively, the TF2 and LRC3 cores exhibited a mean core shear strengths of 3.63 and 2.40 MPa, respectively with a standard deviations of 0.1 MPa for both. The XF6, TF2, and LRC3 cores all passed for normality using the Anderson-Darling normality test (p-value = 0.38, 0.61, 0.41, respectively). A two-sample t-test comparing the XF6 core to the TF2 core found that the mean core shear strengths were statistically different (p-value < 0.001). A 95% confidence interval showed that the mean core shear

strength of the TF2 core was 0.80-0.99 MPa greater than that of the XF6 core. Similarly, the mean core shear strength of the LRC3 and the XF6 cores was also found to be statistically different ($p\text{-value} < 0.001$). However, with great confidence the XF6 core was found to outperform the LRC3 core by 0.24-0.43 MPa (95% confidence interval).

Only samples that failed due to transverse core shear failure, explosive core failure, or core-to-facing failure were included when determining the mean core shear strength (Figure 20). The XF6 samples all failed due to explosive core failure; however three of the TF2 samples and nine of the LRC3 samples experience a facing failure before a core failure (Figure 21).

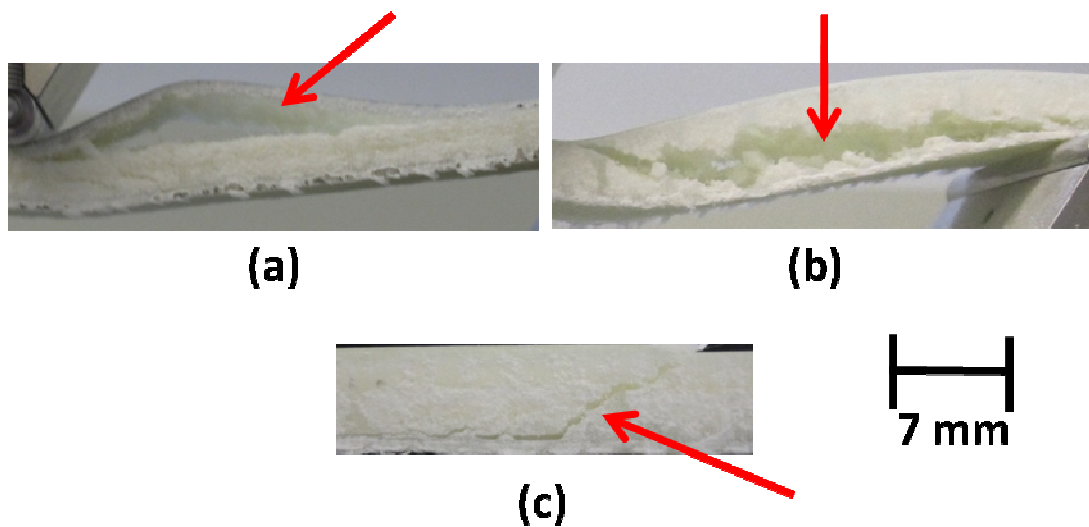


Figure 20: Side view of the three acceptable failure modes observed during the core shear testing: (a) core-to-facing failure; (b) explosive core failure; (c) transverse core shear failure. Red arrows denote failure locations.



Figure 21: Top view photograph of a LRC3 core that experienced a facing failure before core failure during the core shear testing. The failure occurred on the top face sheet directly under the loading nose.

Since a facing failure does not measure the strength of the core, these samples were omitted from the results. The samples that experienced explosive and transverse shear failure modes also exhibited bottom face sheet core-to-facing failure which can be seen in Figure 20 (b & c). The bottom core-to-facing failure was assumed to follow the explosive or transverse core shear failure. In addition, a post-failure inspection of the TF2 samples revealed that approximately 60% of the samples had some type of facing failure in addition to the core failure; it was also assumed that the facing failure in these samples occurred after the core failure. However, due to the rapid nature of the failures it was difficult to confirm these assumptions. A Pareto chart was generated to graphically represent the various failure modes experienced by the TF2 (Figure 22) and LRC3 samples (Figure 23).

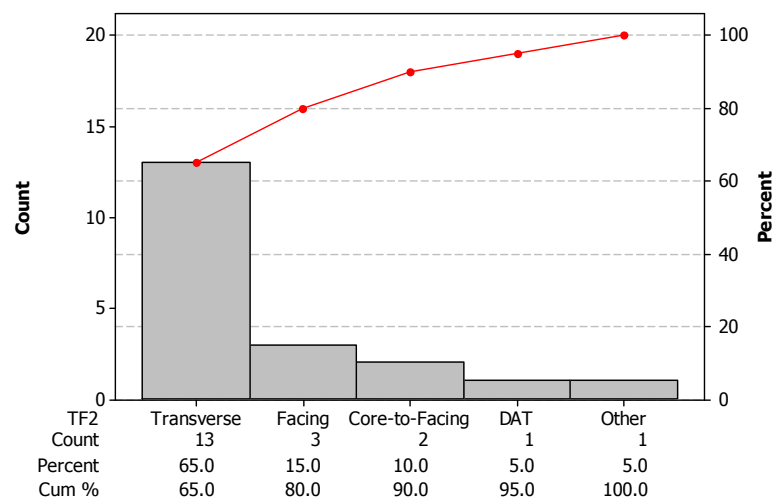


Figure 22: Pareto chart displaying the failure modes experienced by the TF2 samples using ASTM C393 failure code. DAT stands for a special failure case in which the core-to-facing failure occurred directly beneath the loading nose.

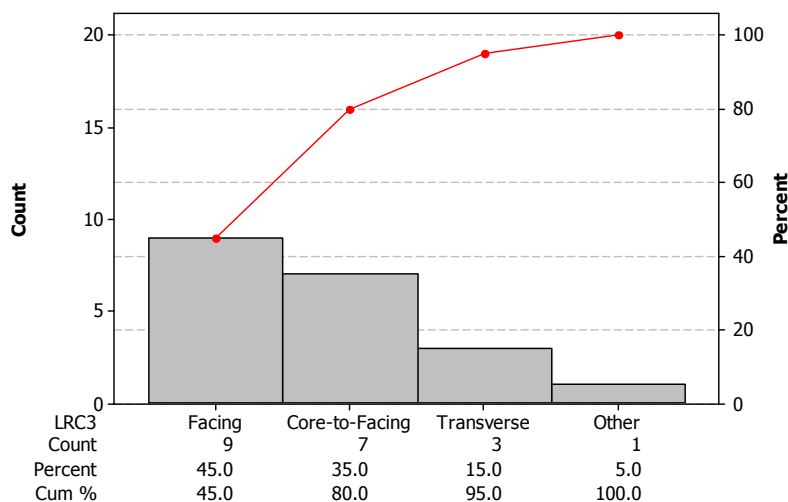


Figure 23: Pareto chart of the failure modes experienced by the LRC3 samples following ASTM C393 failure code.

As mentioned before, the LRC3 samples consisted of two LRC3 cores stacked on top of each other, while the TF2 samples were composed of a TF2 core on top of a LRC4 core. When performing a post-failure inspection of the TF2 and the LRC3 samples that experienced transverse failure, the samples appeared to fail at the interface between the two core materials.

3.2.2 Flexural Modulus Results

The flexural modulus was calculated as a substitute for the core shear modulus from the first linear region experienced by the core shear samples. Since the flexural modulus was not one of the properties initially requested by Aptera, they did not have a baseline database with which to compare the results. Unlike the core shear strength calculations, all samples tested, regardless of failure mode, were included when determining the mean flexural modulus (Figure 24).

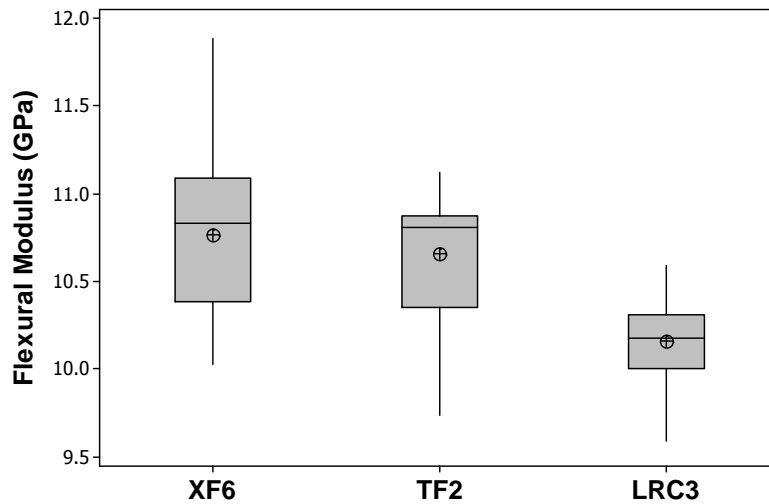


Figure 24: Comparison of the three cores' flexural modulus. The crosshair represents the mean flexural modulus.

The XF6 core exhibited a mean flexural modulus of 10.8 GPa with a standard deviation of 0.48 GPa. The TF2 core had a mean flexural modulus of 10.7 GPa (StDev = 0.36 GPa) while the LRC3 core exhibited a flexural modulus of 10.2 GPa (StDev = 0.26 GPa). All samples passed the Anderson-Darling normality test (p-value = 0.76, 0.09, 0.61, respectively). A two-sample t-test found that there was no statistical difference between the mean flexural moduli of the XF6 and TF2 cores (p-value = 0.43). However, a statistical difference did exist between the mean flexural modulus of the XF6 and LRC3 cores (p-value < 0.001). The XF6 core was found to have a mean flexural modulus that was 0.35-0.97 GPa greater than the LRC3 core (95% confidence interval).

3.2.3 Core Density Calculations

Similar to the calculations performed in the fabric validation results, the mass per surface area was found for the three cores characterized. The completed sandwich core composite's length and width were measured in three locations and divided by the total mass of the sample to determine the mass per surface area. Table VI summarizes the results found.

Table VI: Mass per Surface Area of the Core Materials Characterized

Core Material	Mass/surface area (g/cm ²)	Specific Strength (MPa/ (g/cm ²))	Specific Modulus (GPa/ (g/cm ²))	Total Mass Difference (kg)
XF6	0.676	4.04	15.98	-
TF2	0.693	5.24	15.44	+ 6.6
LRC3	0.632	3.78	16.14	- 16.2

The LRC3 core was found to have the lowest mass per surface area which was expected due to Lantor advertising the material as a “low resin uptake” core¹⁶. The low density of the core resulted in it having the largest specific flexural modulus, even though it had the lowest mean flexural modulus of the three cores. The total mass difference was calculated by assuming the vehicle contained 400 ft² of composite material. The TF2 core would cause a 6.6 kg or 2.6% weight increase in the vehicle's body over the current XF6 core, whereas the LRC3 core would result in a 16.2 kg (6.5%) weight reduction compared to the XF6 core.

3.3 Scanning Electron Microscopy Results

Fractured tensile samples containing Vectorply and Saertex fibers were observed with a scanning electron microscope at high vacuum to qualitatively compare the adhesion between the epoxy matrix and the fractured fiber surfaces. Due to charging of the samples, obtaining images proved difficult. However, a few images were captured of the fractured fiber surfaces (Figure 25).

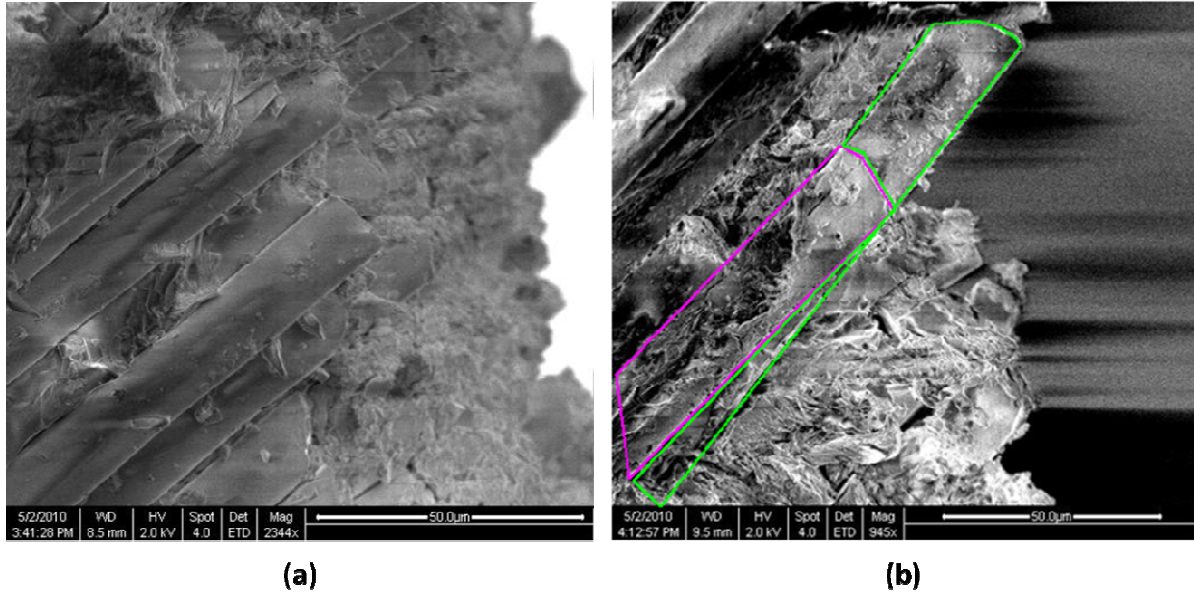


Figure 25: SEM micrographs of epoxy matrix composite containing E-glass fibers: (a) Vectorply fibers (b) Saertex fibers. The Saertex fibers are outlined in green and purple to better identify them.

The SEM micrograph of the Vectorply fiber showed a clean surface (Figure 25 (a)) indicating poor wettability and a lack of adhesion between the fiber and the epoxy matrix. Conversely, the SEM micrograph of the Saertex fiber showed a surface that was littered with matrix material suggesting greater adhesion at the fiber-matrix interface. These results correlate with the mechanical properties observed during testing, Saertex fabrics outperformed Vectorply fabrics.

4. Discussion

Saertex fabrics were shown to outperform Vectorply fabrics in all mechanical properties characterized (Table VII).

Table VII: Summary of Vectorply and Saertex Mechanical Properties

Mechanical Property	Vectorply Fabric	Saertex Fabric	Difference in Means ($\mu_{\text{Saertex}} - \mu_{\text{Vectorply}}$)
Tensile Strength (MPa)	285	302	6.7 - 28.9
Tensile Modulus (GPa)	16.8	17.7	0.29 - 1.47
Short-Beam Strength (MPa)	40.8	46.8	4.6 - 7.3
In-plane Shear Strength (MPa)	40.88	74.95	32.1 - 36.0
Mass / Surface Area (g/cm ²)	0.36	0.34	-

Both companies have the same amount of E-glass fiber present in their fabric (36 oz.), consist of a quadraxial weave in a [0°, +45°, 90°, -45°] orientation, are embedded within an identical epoxy matrix, have equal fiber diameters, and consist of the same volume fraction of E-glass fibers (0.60). Both fabric suppliers also employ a polyester stitch technique to secure the layers of the fabric together and prevent damage experienced by fibers in woven fabrics due to crimping¹⁷. Through visual observations, the stitching technique varied between the two fabrics, but how the stitching effects the mechanical properties of the resulting laminate could not be quantified.

The major difference between the two fabric suppliers is the use of a different PPG fibers (Saertex's fabrics utilized the newer Hybon 2026 fibers while Vectorply's fabrics consisted of the Hybon 2022 fibers). To determine why a difference existed between the two fabric suppliers, scanning electron microscopy was utilized to qualitatively compare the adhesion between the fibers and the surrounding epoxy matrix.

The SEM micrographs revealed that the Saertex fibers contained a greater amount of epoxy matrix on the fiber surface compared to the Vectorply fibers. Fiber manufacturers typically apply a fiber surface treatment (in the form of a sizing) to improve fiber surface wettability with the matrix material, thus creating a stronger bond at the fiber-matrix interface. Fiber surface treatments are also used to protect the fiber surface from reactive fluids and moisture⁸. Both of the fabric supplier's fibers contained a protective sizing that consisted of a organofunctional silicon compounds, otherwise known as a silane (Figure 26).

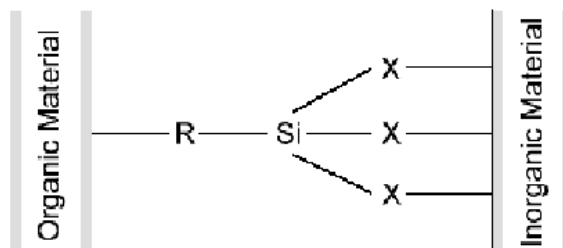


Figure 26: Silane coupling agent that has a silicon bonded to a functional group (R) which is compatible with the epoxy matrix. The inorganic material is the E-glass fiber, while the organic material is the epoxy resin⁸.

The functional group (R) in the silane film reacts with the epoxy resin to form a chemical bond between the fibers and the matrix. Depending on the epoxy matrix, different functional groups can have various degrees of compatibility⁸. The exact chemical composition of the sizing used on the tested fabrics is considered proprietary to PPG and was not identified. However, PPG has stated that the newer fibers (2026 fibers) have a different silane sizing compare to the older fibers (2022 fibers). The new sizing has been shown to improve mechanical properties by approximately 10%²⁶.

The SEM micrographs of the Vectorply fiber showed a weak fiber-matrix coupling effect which was characterized by the “clean” fiber surfaces and the appearance of impressions at the fiber-matrix interface due to debonding of the fiber from the matrix. Conversely, the Saertex fibers had a coating of the epoxy matrix and no observed debonding between the fiber and the matrix at the fracture surface. It should be noted that with a poor coupling agent or no coupling agent, stress transfer between the fibers and the matrix can still exist due to mechanical interlocking that occurs during polymerization shrinkage and thermal contraction of the matrix during curing. However, at high loads the difference in expansion of the fibers and the matrix can relieve the mechanical interlocking and cause the laminate to fail⁸.

A stronger interfacial bond created between the fibers and the matrix results in a better transfer of shear stresses between the matrix and the fibers. This subsequently improves the tensile strength as well as interlaminar shear strength (short-beam strength) of the composite⁸. The SEM observations support the mechanical results; Saertex outperformed Vectorply in short-beam strength, tensile strength and tensile modulus. These results also correlate with PPG’s claims that their new fibers (2026), which were used in the Saertex fabrics, exhibit superior mechanical properties to their older fibers (2022) which were used in the Vectorply fabrics. It should be noted that Saertex believes the increase in

mechanical properties was due to the superior handling of the fibers during the stitching of the fabric¹⁷. However, since the two fabric suppliers used different fiber inputs this claim could not be verified.

The large difference in in-plane shear strength was thought to be caused by external factors outside of the supplier. The fabrication process used to create all the PMC samples consisted of laying down the fabrics and vacuum bag by hand and then using a portable vacuum system to assist the flow of the resin throughout the matrix. Since the in-plane shear test relies on the composite consisting of a [+45°/-45°] laminate, small movements during the resin infusion process could cause some of the fabrics to rotate and become aligned with the tensile axis. The first set of samples tested, Vectorply, only contained two fabrics of biaxial weave, thus the probability of the fabrics rotating a significant amount was small. Conversely, the second set of samples tested, Saertex, consisted of four layers of the biaxial weave. Ensuring that all the fabrics are aligned would be more difficult in four layers of fabric compared to two. This could cause the laminate to have fibers that would be experiencing a normal force component as opposed to a pure shear component experienced at a 45° angle, thus causing the laminate to carry a larger load and have an in-plane shear strength that was larger than expected. However, the orientation of the fibers within each ply was not characterized and thus the above claims could not be validated.

The difference in core shear strength between the three cores was attributed to the amount of resin uptake during the fabrication process of the panels. The LRC3 core, which consisted of two LRC3 cores stacked on top each other, experienced only facing and core-to-facing failures. As mentioned, Lantor advertises the LRC series as a low resin uptake core material due to fewer resin flow channels per surface area over their XF series of cores. The adhesion between the core and the face sheets is due to the interface created by the epoxy resin. Less epoxy resin uptake would create weaker adhesion between the face sheet and core causing it to fail at that location.

The TF2 core, which consisted of a layer of TF2 bonded to a layer of LRC4 core, exhibited the largest mean core shear strength (3.6 MPa) and also had the largest mass per surface area ratio. The greater amount of resin uptake, which was confirmed by the increase in density compared to the other cores, resulted in a better adhesion between the core and face sheets thus causing the material to fail within the core as opposed to a core-to-facing failure. As noted in the results section, the B surface of the TF2 samples experienced core-to-facing failure following the transverse shear failure. The B surface was the surface that was in contact with the LRC4 core which could explain why a core-to-facing failure was occurring on the B surface instead of the A surface. An attempt was made to characterize the concentration of resin contained at the core-face sheet interface by mounting the composite in acrylic

and examining the surface in cross-section with an optical microscope. However, due to plastic smearing of the core during polishing and cutting, discernable photographs could not be captured.

5. Conclusions

1. Laminates containing Saertex's fabric exhibited statistically superior mechanical properties compared to laminates with Vectorply's fabric and thus Saertex was found to be a valid fabric supplier for use in Aptera's composite system.
2. The difference in mechanical properties between the two suppliers was attributed to the greater adhesion at the fiber-matrix interface observed in the Saertex fibers compared to the Vectorply fibers.
3. The TF2 core exhibited the greatest mean core shear strength (3.62 MPa) compared to Aptera's current core (XF6 = 3.2 MPa) and alternate core (LRC3 = 2.8 MPa). However, a sandwich composite containing the TF2 core exhibited the largest weight per surface area (0.69 g/cm²).
4. The difference in core shear properties was attributed to the different amount of resin uptake of the cores.

6. Recommendations

In order to finish the validation process of Saertex fabrics and the characterization of the alternate core materials the following measures should be taken:

- Validate the in-plane shear modulus and compressive strength of laminates containing Saertex fabrics.
- Conduct in-plane shear strength tests on laminates of the same thickness to determine if a discrepancy between the two fabrics still exist.
- Perform mechanical testing on Vectorply laminates that employ PPG's Hybon 2026 fibers and compare to Saertex's fabric.
- Determine core shear modulus of the two alternate core materials using ASTM C273 as opposed to ASTM C393.
- Characterize epoxy resin content at the interface of the core and the face sheets.

7. Work Cited

- ¹ Aptera Motors. Aptera. Web. 07 Dec. 2009. <http://www.aptera.com>
- ² Money, Bruce. "Everything but the Engine." *Automotive Engineering International* July 2009: 10-13. Print.
- ³ Squatriglia, Chuck. "We Drive the Aptera, and It's a Real Car." *Wired* 21 Apr. 2009. Print.
- ⁴ "Retail Prices for Regular Gasoline." *US Energy Information Administration*. Web. 31 Jan. 2010. <http://tonto.eia.doe.gov/dnav/pet/pet_pri_gnd_a_epmr_pte_cp_gal_w.htm>.
- ⁵ Brooke, Lindsay. "A Featherweight Future." *Automotive Engineering International* May 2009: 24-27. Print.
- ⁶ Vlasic, Bill, and Nick Bunkley. "Hazardous Conditions for the Auto Industry." *The New York Times* 1 Oct. 2008, New York ed., C1 sec. Print.
- ⁷ Anderson, Krista. Personal interview. 2 Dec. 2009, 28 Apr. 2010, 5 May 2010.
- ⁸ Mallick, P.K. *Fiber-Reinforced Composites Materials, Manufacturing, and Design*, Second Edition (Dekker Mechanical Engineering). CRC, 1993. Print. p. 1-5; 15-24; 69-72; 212-216.
- ⁹ Daniel, Isaac, and Ori, Ishai. *Engineering Mechanics of Composite Materials*. 2nd ed. New York: Oxford UP, 2006. Print. p. 38-40; 380-382.
- ¹⁰ Shalin, R. E. *Polymer Matrix Composites*. London, Angleterre: Chapman and Hall, 1995. Print. p. 1-3.
- ¹¹ Zhandarov, Serge, and Mader. "Characterization of Fiber/Matrix Interface Strength: Applicability of Different Tests, Approaches and Parameters." *Composites Science and Technology* 65 (2005): 149-60. *Science Direct*. Web.
- ¹² Ashley, Steven. "Light Weighting Gives Composites New Life." *Automotive Engineering International* Aug. 2009: 34-37. Print.
- ¹³ "Congress Boosts Vehicle Fuel-Efficiency Mandate." *NPR*. NPR, 18 Dec. 2007. Web. 14 Oct. 2009. <<http://www.npr.org/templates/story/story.php?storyId=17366844>>.
- ¹⁴ "Product Nomenclature." *Vectorply*. Web. 15 Mar. 2010. <<http://vectorply.com>>.
- ¹⁵ PPG. *Technical Data Sheet- Hybon 2022 Roving*. PPG Fiber Glass. Web. 1 June 2010.

-
- ¹⁶ "Lantor.nl - Lantor Soric® Flexible Core." *Lantor.nl - Lantor B.V.* Web. 18 May 2010.
<http://www.lantor.nl/index.php/id_structuur/10599/soric.html>.
- ¹⁷ Kissinger, Christian (Saertex Composite Engineer). Personal interview. 28 May 2010.
- ¹⁸ PPG. Technical Data Sheet- Hybon 2026 Roving. *PPG Fiber Glass*. Web. 1 June 2010.
- ¹⁹ *ASTM D 3039M: Standard Test Method for Tensile Properties of Polymer Matrix Composite Materials*. 2008, ASTM. p. 79-91.
- ²⁰ Carlsson, Leif A. *Experimental Characterization of Advanced Composite Materials*. Englewood Cliffs, N.J.: Prentice-Hall, 1987. Print. p. 77-80.
- ²¹ *ASTM D3518: Standard Test Method for In-Plane Shear Response of Polymer Matrix Composite Materials by Tensile Test of a +/- 45° Laminate*. 2007, ASTM. p. 124-130.
- ²² *ASTM D 2344M: Standard Test Method for Short-Beam Strength of Polymer Matrix Composite Materials and Their Laminates*. 2006, ASTM. p. 71-78.
- ²³ *ASTM C 393M: Standard Test Method for Core Shear Properties of Sandwich Constructions by Beam Flexure*. 2006, ASTM. p. 1-8.
- ²⁴ *ASTM D 7250: Standard Practice for Determining Sandwich Beam Flexural and Shear Stiffness*. 2006, ASTM. p. 560-566.
- ²⁵ Devore, Jay, and Nicholas R. Farnum. *Applied Statistics for Engineers and Scientists*. Belmont, CA: Thomson Brooks/Cole, 2005. Print.
- ²⁶ Bolton, Michael (Vectorply Composite Engineer). Personal interview. 1 Jun. 2010.